JSHC
Japan Society of Histochemistry and Cytochemistry
Established 1959

Acta Histochem. Cytochem. 46 (5): 137–143, 2013
doi:10.1267/ahc.13007

Differential Increases in the Expression of Intermediate Filament Proteins and Concomitant Morphological Changes of Transdifferentiating Rat Hepatic Stellate Cells Observed *In Vitro*

Yoshihiro Mezaki[1], Mayako Morii[2], Taku Hebiguchi[2], Kiwamu Yoshikawa[1], Noriko Yamaguchi[1], Mitsutaka Miura[1], Katsuyuki Imai[1], Hiroaki Yoshino[2] and Haruki Senoo[1]

[1]Department of Cell Biology and Morphology, Akita University Graduate School of Medicine, 1–1–1 Hondo, Akita 010–8543, Japan and [2]Department of Pediatric Surgery, Akita University Graduate School of Medicine, 1–1–1 Hondo, Akita 010–8543, Japan

Received March 4, 2013; accepted August 30, 2013; published online October 23, 2013

The primary function of hepatic stellate cells (HSCs) is the storage of vitamin A. However, they are also responsible for liver fibrosis and are therapeutic targets for treatment of liver cirrhosis. Among the many molecular markers that define quiescent or activated states of HSCs, the characteristics of type III intermediate filaments are of particular interest. Whereas vimentin and desmin are upregulated in activated HSCs, glial fibrillary acidic protein is downregulated in activated HSCs. The functional differences between vimentin and desmin are poorly understood. By time-course quantifications of several molecular markers for HSC activation, we observed that the expression of vimentin preceded that of desmin during the transdifferentiation of HSCs. The immunoreactivity of vimentin in transdifferentiated HSCs was more intense in perinuclear regions compared to that of desmin. We propose that the delayed expression of desmin following the expression of vimentin and the peripheral localization of desmin compared to vimentin are both related to the more extended phenotype of transdifferentiating HSCs observed *in vitro*.

Key words: hepatic stellate cell, intermediate filament, vimentin, desmin, myofibroblast

I. Introduction

Hepatic stellate cells (HSCs), also referred to as vitamin A storing cells, Ito cells or lypocytes, reside in the space between hepatocyte cell cords and liver sinusoidal endothelial cells and store large amounts of vitamin A [24]. After the discovery that HSCs are the primary site of collagen synthesis [5, 22], HSCs became a promising therapeutic target for treatment of liver fibrosis [7]. During liver fibrosis, quiescent HSCs transdifferentiate or activate to actively proliferating myofibroblastic cells [6].

Many molecular markers define the quiescent and activated states of HSCs *in vitro* and *in vivo*. For example, the compositions and amounts of intermediate filaments change variably depending on the site of the hepatic lobule *in vivo* and on activation states both *in vivo* and *in vitro*. Intermediate filaments were named due to their characteristic ten nm diameter, a size between those of actin filaments (six nm) and microtubules (25 nm) [12]. Among the three types of cytoskeletal filaments within the cell, intermediate filaments possess the most stable architecture. They are resistant to both nonionic detergents and high-salt buffers and remain in a polymerized state even during mitosis [9, 15]. The number of genes encoding intermediate filaments was estimated to be about 70 in humans and have been classified into families I to V [11, 14]. HSCs express at least three type III intermediate filaments (vimentin, desmin and glial fibrillary acidic protein (GFAP)) and a type IV intermediate filament (nestin) [20]. A type III intermediate filament, desmin, is a marker for both quiescent and activated HSCs *in vivo* [1, 26]. Desmin immuno-

Correspondence to: Yoshihiro Mezaki, Ph.D., Department of Cell Biology and Morphology, Akita University Graduate School of Medicine, 1–1–1 Hondo, Akita 010–8543, Japan.
E-mail: mezaki@gipc.akita-u.ac.jp

reactivity is more prominent in periportal HSCs compared to pericentral HSCs [2, 19, 25]. In cultured HSCs, however, it was reported that desmin expression increased during activation [20]. Another type III intermediate filament, vimentin, is also a marker for HSCs [4] and is upregulated in cultured HSCs [20]. On the other hand, GFAP is a marker for quiescent HSC *in vivo* [8] and is downregulated during transdifferentiation *in vitro* [20].

The biological significance of the variation of composition and amounts of intermediate filaments in quiescent and transdifferentiated HSCs is not fully understood. Geerts *et al.* reported an analysis of intermediate filaments using knockout mice. They found that the presence of vimentin is a prerequisite for normal desmin intermediate filament formation in HSCs [10]. Desmin expression is believed to be related to the acquisition of the contractile phenotype in transdifferentiated HSCs, a phenotype that controls the microcirculation within the liver lobule [13].

In this paper, we used confocal microscopic techniques to analyze the subcellular location of vimentin and desmin intermediate filaments in culture-activated rat HSCs. We also characterized the time-course of expression of these proteins. We propose that the more extended morphology of transdifferentiated HSCs might be related to changes of intermediate filament components in the cells.

II. Materials and Methods

Preparation of HSCs

Protocols for animal experimentation were approved by the Animal Research Committee, Akita University Graduate School of Medicine. All animal experiments adhered to the Guidelines for Animal Experimentation of the University. Male Wistar rats, eight weeks of age (weighing 220 to 240 g), were purchased from CLEA Japan (Tokyo, Japan) and used for isolation of HSCs, following the procedure described previously [17, 23]. Livers were first perfused with preperfusion buffer free of calcium and magnesium ions, and then with perfusion buffer containing bacterial collagenase (Wako Pure Chemical, Osaka, Japan) and calcium ions. Dispersed cells were centrifuged at low speed to remove the pelleted parenchymal cells. The supernatant containing non-parenchymal cells was further purified by density gradient centrifugation with Percoll/RediGrad (GE Healthcare Bio-Sciences, Piscataway, NJ, USA), and the layer containing HSCs was seeded on uncoated polystyrene dishes with Dulbecco's modified Eagle Medium, Low Glucose (Life Technologies, Carlsbad, CA, USA) supplemented with 10% fetal bovine serum (SAFC Bioscience, Lenexa, KS, USA).

Western blotting

HSCs cultured on polystyrene dishes were lysed with RIPA buffer (Sigma-Aldrich, St. Louis, MO, USA), which was composed of 50 mM Tris-HCl, pH 8.0, 150 mM sodium chloride, 1.0% Nonidet P-40, 0.5% sodium deoxycholate and 0.1% sodium dodecyl sulfate. In order to avoid protein degradation during preparation of the lysates, prechilled RIPA buffer containing complete protease inhibitor cocktail (Roche Diagnostics, Meylan, France) was applied directly onto the polystyrene dishes. After five min on ice, cells were scraped and lysates (including cell debris) were stored at –85°C. The stored lysates were cleared by centrifugation and protein concentrations were measured with the BCA Protein Assay Kit (Pierce, Rockford, IL, USA). Ten μg of cell lysates were separated by sodium dodecyl sulfate-polyacrylamide gel electrophoresis (SDS-PAGE), and transferred to a polyvinylidene difluoride membrane (Atto, Tokyo, Japan). Nonspecific binding was blocked by 5% skim milk in phosphate buffered saline (PBS) supplemented with 0.1% Tween 20 (Merck, Darmstadt, Germany) (PBST). Membranes were incubated with primary antibodies against vimentin (mouse monoclonal, two μg/ml, M0725, Dako, Glostrup, Denmark), desmin (mouse monoclonal, 4.53 μg/ml, MAB1698, Merck Millipore, Billerica, MA, USA) in PBST for one hr at room temperature. After washing, the secondary antibodies (peroxidase-conjugated AffiniPure goat anti-mouse IgG (H+L) (115-035-003, Jackson ImmunoResearch, West Grove, PA, USA)) were applied to the membranes at a dilution of 1 : 5,000 in PBST for 30 min at room temperature. Bound antibodies were detected by ECL chemiluminescence (GE Healthcare Bio-Sciences), and signals were recorded on X-ray film (Fujifilm, Tokyo, Japan).

Immunocytochemistry

HSCs were cultured on uncoated polystyrene dishes for seven days and were then subcultured on poly-L-lysine-coated glass-bottom dishes (Matsunami Glass, Osaka, Japan) for an additional two to four days. Cells were washed and fixed with 2% (w/v) paraformaldehyde in 100 mM phosphate buffer, pH 7.4, for ten min at room temperature and then treated either with 100% methanol for ten min at –20°C (Fig. 3) or with 0.1% Triton X-100 in PBS for 10 min at room temperature (Figs. 4, 5) for permeabilization. Nonspecific binding was blocked by incubating cells with 1% bovine serum albumin (BSA) (Sigma-Aldrich) in PBS for 30 min at room temperature. Cells were then incubated with anti-desmin antibody (mouse monoclonal, 45.3 μg/ml, MAB1698, Merck Millipore) in PBS plus 1% BSA for one hr at room temperature. After washing, cells were treated with a 1 : 100 dilution of Alexa Fluor 555 donkey anti-mouse IgG (H+L) (A-31570, Life Technologies) in PBS plus 1% BSA for 30 min at room temperature. After desmin staining, cells were incubated with anti-vimentin antibody (goat polyclonal, ten μg/ml, sc-7557, Santa Cruz Biotechnology, Santa Cruz, CA, USA) in PBS plus 1% BSA for one hr at room temperature. After washing, Alexa Fluor 488 donkey anti-goat IgG (H+L) (1 : 100 dilution, A-11055, Life Technologies) was added for 30 min at room temperature. Cells were washed and observed with an LSM510 Laser Scanning Microscope (Carl Zeiss, Jena, Germany).

When cells were stained with BODIPY 493/503

(Life Technologies) to visualize lipid droplets, Alexa Fluor 633 donkey anti-goat IgG (H+L) (1 : 100 dilution, A-21082, Life Technologies) was used for vimentin visualization. When cells were stained with Alexa Fluor 546 phalloidin (A-22283, Life Technologies), Alexa Fluor 633 donkey anti-goat IgG (H+L) and Alexa Fluor 488 donkey anti-mouse IgG (H+L) (1 : 100 dilution, A-21202, Life Technologies) were used to visualize vimentin and desmin, respectively.

Cytochalasin treatment

Cytochalasin treatment was performed as described previously [18].

Morphometry of HSCs

HSCs were observed with an IX70 inverted microscope (Olympus, Tokyo, Japan) and digital images were recorded using a DP70 digital microscope camera (Olympus). Morphometry of HSCs was performed using ImageJ software (NIH, Bethesda, MD, USA) and the area occupied by a cell was measured. Ten cells were used to calculate the occupied area for each day. Quantification of distributions of vimentin, desmin, lipid droplets and mitochondria within the cytoplasm was performed using ImageJ software. Ten lines spanning from the nuclear membrane to the plasma membrane were drawn randomly within a cell. Each line was evenly divided into ten segments and staining intensities in each segment were added together and expressed as percentages. Ten cells were used to calculate distributions of desmin, vimentin, lipid droplets and mitochondria.

Western blotting signal quantification

Western blots signals were captured on X-ray film, and they were scanned with a GT-X800 (Seiko Epson, Nagano,

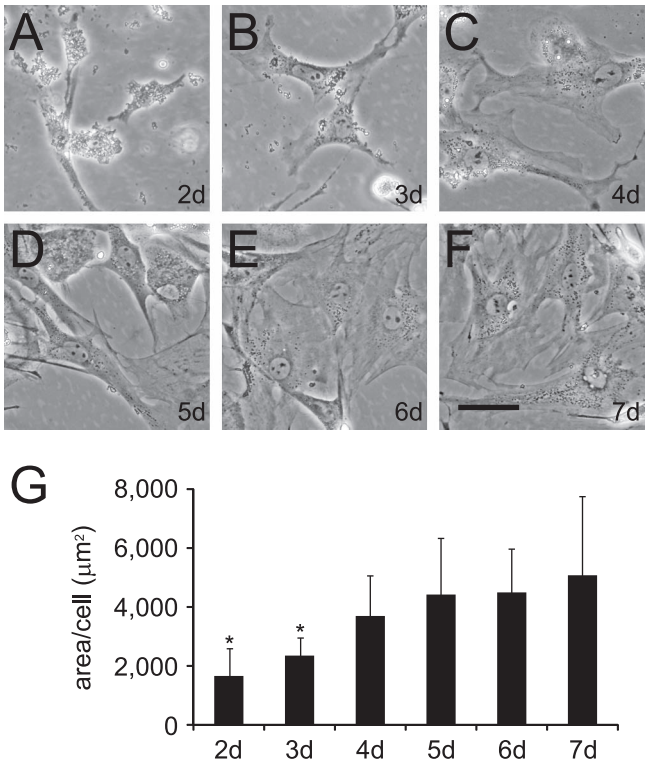

Fig. 1. Morphological changes of rat hepatic stellate cells (HSCs) cultured *in vitro*. (**A–F**) Male Wistar rats at the age of eight weeks were sacrificed for isolation of HSCs as described in Materials and Methods. Cells were cultured on uncoated polystyrene dishes and observed daily by phase contrast microscopy. Bar in panel **F** represents 50 μm and applies to all the panels in this figure. (**G**) The area occupied by a cell was measured. Ten cells were used to calculate the occupied area for each day. Asterisks indicate significant ($P<0.05$) differences compared to day seven by ANOVA.

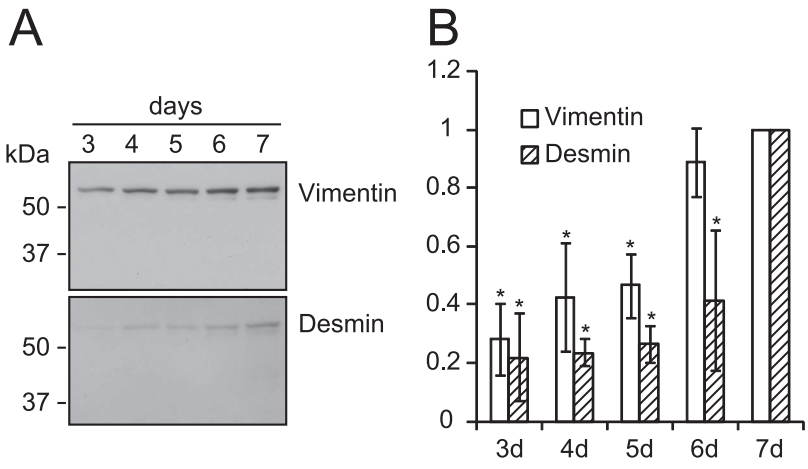

Fig. 2. Expression of vimentin and desmin proteins in transdifferentiating rat HSCs. (**A**) HSCs were collected after the indicated number of days in culture and ten μg of RIPA-soluble cell lysates were separated by SDS-PAGE. Protein expression was assessed by Western blotting. Approximate molecular weights are indicated on the left of the panels. (**B**) The same experiments shown in panel **A** were done at least three times using other lots of HSCs. The intensities of chemiluminescent signals are indicated by means±standard deviations. The signal intensities on day seven were set to one for each protein analyzed. Asterisks indicate significant ($P<0.05$) differences compared to proteins on day seven by ANOVA.

Japan) with linear mode and quantified using ImageJ software. At least three independent lots of HSCs were used for the quantification of Western blotting signals. The signal intensities on day seven were set to one for each protein analyzed.

Statistical analyses

Data analyses were performed using EXCEL software (Microsoft, Redmond, WA, USA) and Hulinks KaleidaGraph software (Synergy Software, Reading, PA, USA). Data are expressed as means±standard deviation. The statistical significance of differences was evaluated by one way analysis of variance (ANOVA) combined with the Tukey test. P values <0.05 were considered to be statistically significant.

III. Results

Morphological changes of rat HSCs activated in vitro

Isolated HSCs plated on uncoated polystyrene dishes spontaneously transdifferentiate, or "activate", to myofibroblast-like cells, as shown in Fig. 1. The areas occupied by HSCs dramatically increased during the first week after seeding (Fig. 1G). At the same time, nuclei with prominent nucleoli became flattened between days two (though they are obscured by cell debris) and four. By days six or seven, most of the HSCs were fully transdifferentiated with stress fibers (composed of actin filaments) in their cytoplasm.

Intermediate filament expression in transdifferentiating rat HSCs

The species and the amounts of intermediate filaments reportedly change during HSC transdifferentiation. Thus, we next analyzed whether the morphological alterations of transdifferentiating HSCs described above correlated with changes in the expression of intermediate filaments. Ten μg of RIPA-soluble whole cell lysates were separated by SDS-PAGE. Protein expression was analyzed by Western blotting (Fig. 2A). Two intermediate filaments, vimentin and desmin, were both upregulated during transdifferentiation of HSCs. The increase in vimentin expression slightly preceded that of desmin (Fig. 2B). The expression of desmin continued to increase until day seven.

Intermediate filament localization in transdifferentiated rat HSCs

We analyzed the intracellular location of desmin and vimentin intermediate filaments in transdifferentiated rat HSCs, using confocal laser scanning microscopy combined with immunofluorescence. As shown in Fig. 3, most of the desmin and vimentin fluorescent signals overlapped. However, vimentin immunoreactivity was more intense in perinuclear regions than peripheral regions of the cytoplasm (Fig. 3B, F, G). As a result, desmin and vimentin showed different distribution patterns within a cell (Fig. 3C, F, G). Many of the transdifferentiated HSCs showed a gradient of expression of the intermediate filaments (Fig. 3E, arrows).

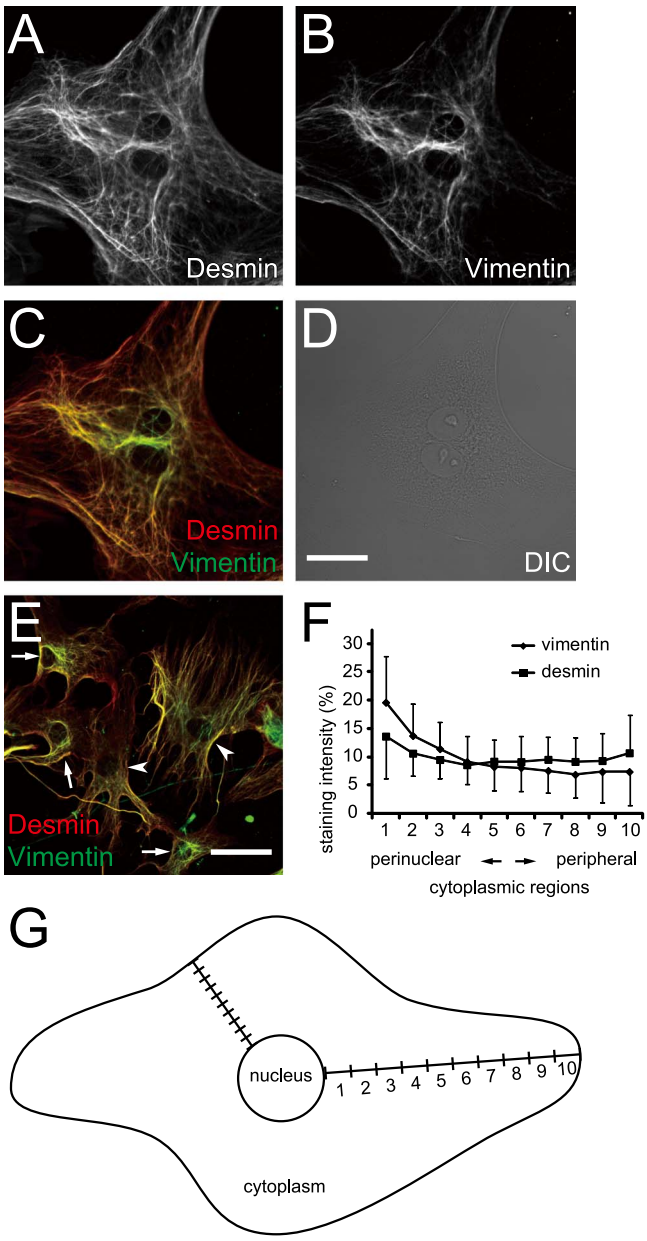

Fig. 3. Immunofluorescent staining of desmin and vimentin in transdifferentiated rat HSCs. HSCs, plated on uncoated polystyrene dishes, were then subcultured on poly-L-lysine-coated glass-bottom dishes and cultured for two additional days. Cells were fixed and stained with mouse anti-desmin and goat anti-vimentin antibodies. Fluorescently-labeled secondary antibodies were used to visualize the locations of desmin (**A**, shown in red in panels **C** and **E**) and that of vimentin (**B**, shown in green in panels **C** and **E**). A differential interference contrast (DIC) image (**D**) is also shown. Bar in panel **D** represents 50 μm and applies to panels **A–D**; the bar in **E** represents 100 μm. Arrows in panel **E** indicate HSCs with prominent perinuclear staining for vimentin in contrast to desmin and arrowheads in panel **E** indicate HSCs with uniform distributions of vimentin and desmin. (**F**) Quantification of cytoplasmic distributions of vimentin and desmin. (**G**) Schema for quantification of distributions of cellular components in a cell. Lines extending from the nuclear membrane to the plasma membrane were drawn. Each line was divided evenly into ten segments from the perinuclear (region 1) to the peripheral (region 10) cytoplasmic regions and staining intensities in each segment were added together and expressed as percentages. Ten lines per cell were drawn and ten cells were used to calculate the distributions.

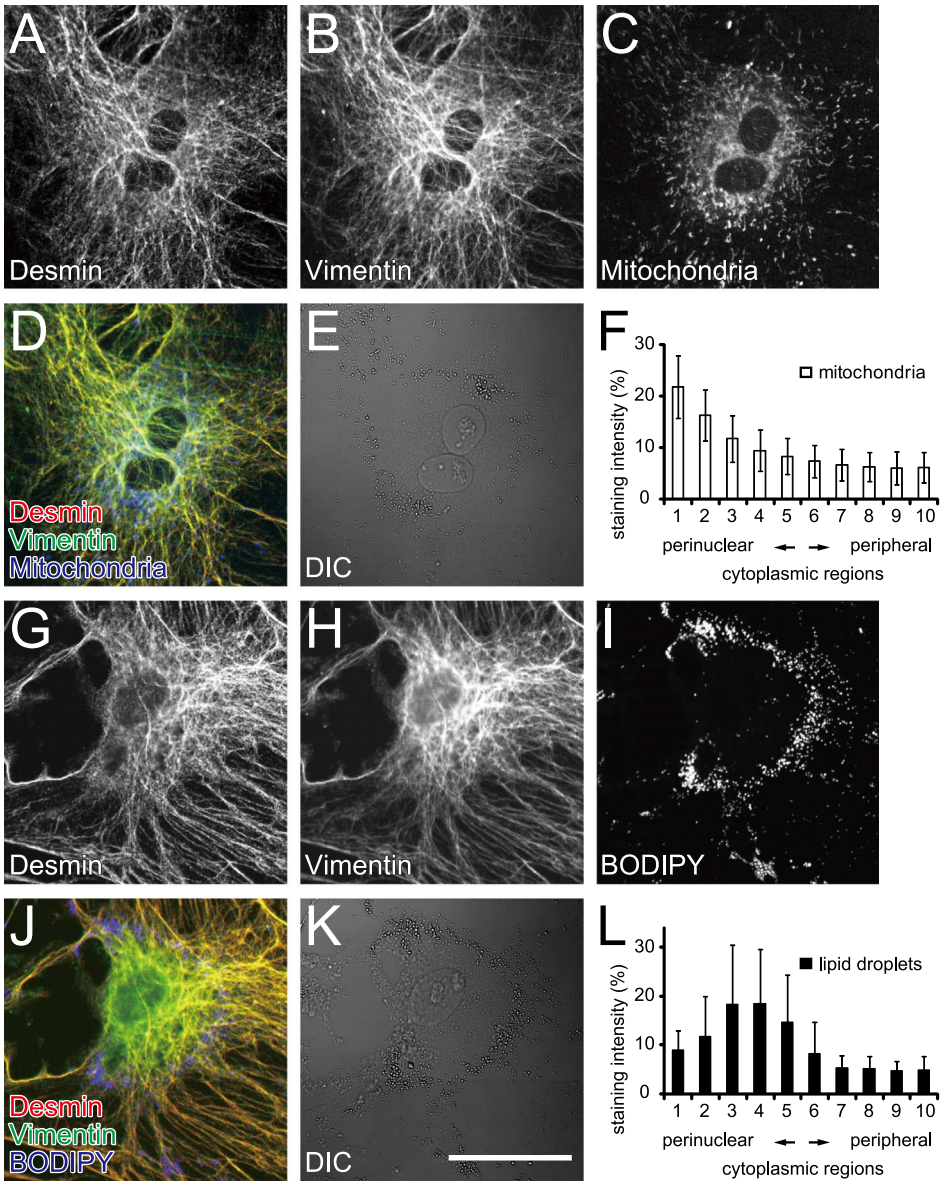

Fig. 4. Distribution of organelles and intermediate filaments. The HSCs plated on uncoated polystyrene dishes were subcultured on poly-L-lysine-coated glass-bottom dishes and cultured for four additional days. Cells were fixed and stained with mouse anti-desmin and goat anti-vimentin antibodies. Fluorescently-labeled secondary antibodies were used to visualize the locations of desmin (**A** and **G**, shown in red in panels **D** and **J**) and that of vimentin (**B** and **H**, shown in green in panels **D** and **J**). Prior to fixation, mitochondria were visualized by using MitoTracker Deep Red 633 (**C**) and shown in blue (**D**). Immediately before observation, lipid droplets were visualized by using BODIPY 493/503 (**I**) and shown in blue (**J**). DIC images (**E** and **K**) are also shown. Bar in panel **K** represents 50 μm and applies to all the panels. (**F** and **L**) Quantification of cytoplasmic distributions of mitochondria and lipid droplets, respectively.

However, some HSCs showed uniform distributions of vimentin and desmin proteins (Fig. 3E, arrowheads).

Distribution of mitochondria and lipid droplets in transdifferentiated rat HSCs

Because intermediate filaments act as a scaffold for cellular organelles [11], we analyzed the distributions of mitochondria and lipid droplets in transdifferentiated rat HSCs and compared them to the locations of desmin and vimentin. As shown in Fig. 4A–F, mitochondria were distributed broadly within the cytoplasm, with a maximum concentration around the nucleus, where vimentin concentration was high (Fig. 3F). On the other hand, lipid droplets stained by BODIPY 493/503, which supposedly contain vitamin A [3, 16], were distributed circumferentially along the line separating perinuclear and peripheral cytoplasmic regions (Fig. 4G–L). Note that lipid droplets revealed by BODIPY 493/503 staining were readily recognizable by differential interference contrast (DIC) microscopy (Fig. 4K).

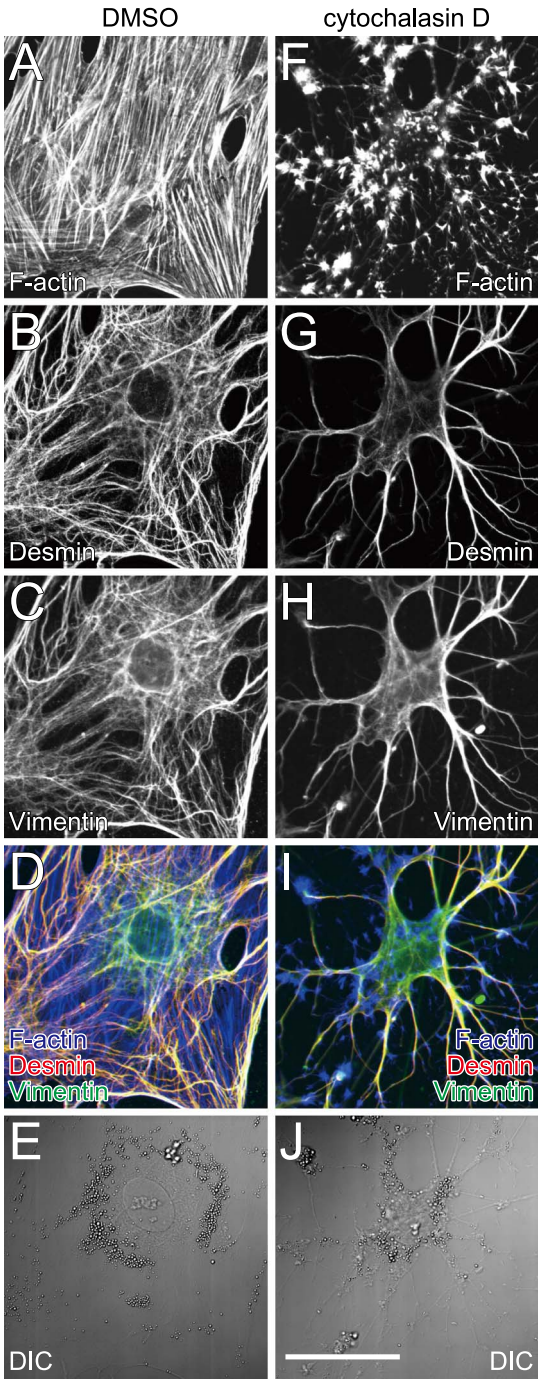

Fig. 5. Effect of stress fiber disruption on desmin and vimentin locations in transdifferentiated rat HSCs. HSCs plated on uncoated polystyrene dishes were subcultured on poly-L-lysine-coated glass-bottom dishes and cultured for three additional days. Activated HSCs were treated with either DMSO (**A–E**) or two μM cytochalasin D (**F–J**) for one h. Cells were then fixed and stained with mouse anti-desmin (**B** and **G**, shown in red in panels **D** and **I**) and goat anti-vimentin (**C** and **H**, shown in green in panels **D** and **I**) antibodies. F-actin was stained by Alexa Fluor 546 phalloidin (**A** and **F**) and shown in blue (**D** and **I**). DIC images (**E** and **J**) are also shown. Bar in panel **J** represents 50 μm and applies to all the panels.

Location of intermediate filaments in cytochalasin-treated transdifferentiated rat HSCs

We analyzed the effect of stress fiber disruption on the locations of desmin and vimentin in transdifferentiated rat HSCs. Cytochalasin D, which is an actin-depolymerizing agent, disrupted the architecture of microfilaments within the HSCs (Fig. 5F–J), changing the extended phenotype of transdifferentiated HSCs to a more contracted phenotype with many cell protrusions surrounded by segmented F-actins. In contrast to the shrinkage of peripheral cytoplasmic regions rich in desmin, the nucleus and perinuclear regions rich in vimentin seemed intact after microfilament disruption by cytochalasin D treatment.

IV. Discussion

It is thought that intermediate filaments act as a scaffold for cellular organelles such as mitochondria, the Golgi complex, microtubule organizing centers, and the nucleus [11]. Intermediate filaments likely play similar roles for mitochondria and lipid droplets in transdifferentiated HSCs (Fig. 4). Disruption of actin polymerization by cytochalasin D resulted in aberrant distributions of vimentin and desmin especially in peripheral regions of HSCs (Fig. 5), presumably due to the detachment of parts of the cell at the peripheral regions. This observation implies that intermediate filaments and actin filaments coordinately establish the morphology of transdifferentiating HSCs.

The reason why HSCs change their intermediate filament components during their activation is totally unknown, due in part to the limited understanding of the functional differences among the different types of intermediate filaments. One intriguing insight into the functional relationship between the different types of intermediate filaments was reported by Geerts *et al.* [10]. They observed that knocking out the gene for either GFAP or vimentin did not affect the amount of desmin but did affect its subcellular location, leading to its perinuclear accumulation. Our observations that increases in the protein levels of vimentin slightly preceded that of desmin (Fig. 2) and that vimentin was enriched in perinuclear regions compared to desmin (Fig. 3) are in good accord with the earlier data and provide additional support for their conclusion that vimentin is required for normal filament formation by desmin. We propose that during transdifferentiation, the change of HSC morphology to a more extended form might be due to the increased proportion of desmin versus vimentin within the cytoplasm, combined with the tendencies of desmin and vimentin to localize to peripheral regions and perinuclear regions, respectively [21]. It would be interesting to investigate whether GFAP, another intermediate filament that is negatively regulated in transdifferentiated HSCs, is involved in the distributions of vimentin and desmin. Thus far, we have not succeeded in detecting GFAP protein either by Western blotting or immunohistochemistry using the HSCs isolated by our method.

V. Acknowledgments

This work was supported by Japan Society for the Promotion of Science Grants-in-Aid for Scientific Research (23790269 to YM, 23792026 to MMo, 24614003 to NY, 23592623 to HY, 23590228 and 24255003 to HS).

VI. References

1. Ballardini, G., Fallani, M., Biagini, G., Bianchi, F. B. and Pisi, E. (1988) Desmin and actin in the identification of Ito cells and in monitoring their evolution to myofibroblasts in experimental liver fibrosis. *Virchows Arch. B. Cell Pathol. Incl. Mol. Pathol.* 56; 45–49.
2. Ballardini, G., Groff, P., Badiali de Giorgi, L., Schuppan, D. and Bianchi, F. B. (1994) Ito cell heterogeneity: desmin-negative Ito cells in normal rat liver. *Hepatology* 19; 440–446.
3. D'Ambrosio, D. N., Walewski, J. L., Clugston, R. D., Berk, P. D., Rippe, R. A. and Blaner, W. S. (2011) Distinct populations of hepatic stellate cells in the mouse liver have different capacities for retinoid and lipid storage. *PLoS. One* 6; e24993.
4. de Leeuw, A. M., McCarthy, S. P., Geerts, A. and Knook, D. L. (1984) Purified rat liver fat-storing cells in culture divide and contain collagen. *Hepatology* 4; 392–403.
5. Friedman, S. L., Roll, F. J., Boyles, J. and Bissell, D. M. (1985) Hepatic lipocytes: the principal collagen-producing cells of normal rat liver. *Proc. Natl. Acad. Sci. U S A* 82; 8681–8685.
6. Friedman, S. L. (2000) Molecular regulation of hepatic fibrosis, an integrated cellular response to tissue injury. *J. Biol. Chem.* 275; 2247–2250.
7. Friedman, S. L. (2010) Evolving challenges in hepatic fibrosis. *Nat. Rev. Gastroenterol. Hepatol.* 7; 425–436.
8. Gard, A. L., White, F. P. and Dutton, G. R. (1985) Extra-neural glial fibrillary acidic protein (GFAP) immunoreactivity in perisinusoidal stellate cells of rat liver. *J. Neuroimmunol.* 8; 359–375.
9. Gard, D. L., Bell, P. B. and Lazarides, E. (1979) Coexistence of desmin and the fibroblastic intermediate filament subunit in muscle and nonmuscle cells: identification and comparative peptide analysis. *Proc. Natl. Acad. Sci. U S A* 76; 3894–3898.
10. Geerts, A., Eliasson, C., Niki, T., Wielant, A., Vaeyens, F. and Pekny, M. (2001) Formation of normal desmin intermediate filaments in mouse hepatic stellate cells requires vimentin. *Hepatology* 33; 177–188.
11. Godsel, L. M., Hobbs, R. P. and Green, K. J. (2008) Intermediate filament assembly: dynamics to disease. *Trends Cell Biol.* 18; 28–37.
12. Ishikawa, H., Bischoff, R. and Holtzer, H. (1968) Mitosis and intermediate-sized filaments in developing skeletal muscle. *J. Cell Biol.* 38; 538–555.
13. Kawada, N., Klein, H. and Decker, K. (1992) Eicosanoid-mediated contractility of hepatic stellate cells. *Biochem. J.* 285; 367–371.
14. Kim, S. and Coulombe, P. A. (2007) Intermediate filament scaffolds fulfill mechanical, organizational, and signaling functions in the cytoplasm. *Genes Dev.* 21; 1581–1597.
15. Lazarides, E. (1982) Intermediate filaments: a chemically heterogeneous, developmentally regulated class of proteins. *Annu. Rev. Biochem.* 51; 219–250.
16. Lee, T. F., Mak, K. M., Rackovsky, O., Lin, Y. L., Kwong, A. J., Loke, J. C. and Friedman, S. L. (2010) Downregulation of hepatic stellate cell activation by retinol and palmitate mediated by adipose differentiation-related protein (ADRP). *J. Cell. Physiol.* 223; 648–657.
17. Mezaki, Y., Yoshikawa, K., Yamaguchi, N., Miura, M., Imai, K., Kato, S. and Senoo, H. (2007) Rat hepatic stellate cells acquire retinoid responsiveness after activation in vitro by post-transcriptional regulation of retinoic acid receptor alpha gene expression. *Arch. Biochem. Biophys.* 465; 370–379.
18. Mezaki, Y., Yamaguchi, N., Yoshikawa, K., Miura, M., Imai, K., Itoh, H. and Senoo, H. (2009) Insoluble speckled cytosolic distribution of retinoic acid receptor alpha protein as a marker of hepatic stellate cell activation in vitro. *J. Histochem. Cytochem.* 57; 687–699.
19. Niki, T., De Bleser, P. J., Xu, G., Van Den Berg, K., Wisse, E. and Geerts, A. (1996) Comparison of glial fibrillary acidic protein and desmin staining in normal and CCl4-induced fibrotic rat livers. *Hepatology* 23; 1538–1545.
20. Niki, T., Pekny, M., Hellemans, K., Bleser, P. D., Berg, K. V., Vaeyens, F., Quartier, E., Schuit, F. and Geerts, A. (1999) Class VI intermediate filament protein nestin is induced during activation of rat hepatic stellate cells. *Hepatology* 29; 520–527.
21. Pinzani, M., Gesualdo, L., Sabbah, G. M. and Abboud, H. E. (1989) Effects of platelet-derived growth factor and other polypeptide mitogens on DNA synthesis and growth of cultured rat liver fat-storing cells. *J. Clin. Invest.* 84; 1786–1793.
22. Senoo, H., Hata, R., Nagai, Y. and Wake, K. (1984) Stellate cells (vitamin A-storing cells) are the primary site of collagen synthesis in non-parenchymal cells in the liver. *Biomed. Res.* 5; 451–458.
23. Senoo, H. and Hata, R. (1993) Isolation of perisinusoidal stellate cells (vitamin A-storing cells, fat-storing cells) of the rat liver. *Connective Tissue* 25; 129–137.
24. Wake, K. (1980) Perisinusoidal stellate cells (fat-storing cells, interstitial cells, lipocytes), their related structure in and around the liver sinusoids, and vitamin A-storing cells in extrahepatic organs. *Int. Rev. Cytol.* 66; 303–353.
25. Wake, K. and Sato, T. (1993) Intralobular heterogeneity of perisinusoidal stellate cells in porcine liver. *Cell Tissue Res.* 273; 227–237.
26. Yokoi, Y., Namihisa, T., Kuroda, H., Komatsu, I., Miyazaki, A., Watanabe, S. and Usui, K. (1984) Immunocytochemical detection of desmin in fat-storing cells (Ito cells). *Hepatology* 4; 709–714.